Compensation of Cross-gain Modulation in Filtered Multi-channel Optical Signal Processing Applications

T. Banwell, A. Agarwal*, P. Toliver, and T.K. Woodward
Telcordia Technologies, Red Bank, New Jersey 07701
**anjali@research.telcordia.com*

Abstract: We experimentally demonstrate compensation of nonlinearity due to cross-gain modulation in wideband analog systems employing narrow-band optical filtering, which is essential for multi-channel optical signal processing in RF channelizer applications.

OCIS Codes: (060.2330) Fiber optics communications; (060.5060) Phase modulation; (060.5625) Radio frequency photonics.

1. Introduction: Input signal channelization is often employed in wideband RF signal processing applications to significantly reduce the bandwidth required for analog-to-digital conversion (ADC). There has been significant progress in integrated optical filters [1] that suggests that optical channelizers can be made for RF signal channelization; optical bandpass filters select a small portion of a modulated optical signal spectrum. In such an electrical-optical-electrical (E/O/E) link, an arbitrary wideband RF signal with multiple frequency components suffers not only from intermodulation distortion (IMD) due to non-linearity, but cross-gain modulation (XGM) effects can be pronounced when multiple signals compete for available optical signal.

We have previously derived an analytical expression for the transfer function of an *optically filtered* phase modulated coherent analog photonic link valid for arbitrary passband RF signals [2]. In this paper, we extend the analysis to *wideband* RF signals with bandwidth larger than the bandwidth of the optical filter, as typically encountered in channelization applications. A number of electronic and optical methods such as predistortion [3] and post-processing [4, 5] have been employed for compensating the intermodulation distortion in photonic analog systems. We show here how the impact of XGM can be mitigated through postdistortion compensation using joint nonlinear estimation. We then experimentally demonstrate for the first time to our knowledge, compensation of nonlinearity due to XGM in such filtered multi-channel photonic systems. Although multi-channel sub-carrier multiplexed (SCM) systems are also constrained by nonlinearity, they generally constrain the modulation depth of individual channels and exploit pre-distortion compensation to extend the useful aggregate modulation depth [6]. Here we demonstrate methods applicable to an optically channelized system.

2. System description: Consider a phase modulated filtered coherent analog multi-channel photonic system as shown in Figure 1(a). The output of a continuous wave (cw) laser is phase modulated by an input RF signal. A Mach-Zehnder modulator biased for carrier suppression is used so that the carrier and all even order sidebands are suppressed. The modulated signal is then optically filtered by a bank of filters to select a portion of the first order upper sideband and reject the higher order harmonics. At the receiver an LO signal is used to coherently downconvert to an intermediate frequency ω_{IF} resulting in the detected electrical signal $S(t)$. An example of XGM distortion effect is shown in Fig.1 (b) that shows the time-domain waveforms for signals in two frequency bands (referred to as signal and interferer) at various power levels of the interferer tones (the signal tones power level is fixed at 0dBm). The signal waveform shows pronounced distortion due to XGM as the interferer power levels are increased, while distortion of the interferer is predominantly due to its own 3rd order intermodulation terms and is not impacted by the weaker signal.

We have previously derived [2] the expression for the recovered signal $S(t)$ for an arbitrary passband input signal $z(t) = \rho(t)\sin(\omega_{rf}t + \vartheta(t))$

$$S(t) \propto J_1(\beta\rho(t))\sin(\omega_{IF}t + \vartheta(t)) \tag{1}$$

where $\beta = \pi / V_\pi$ and $J_1(.)$ is the first order Bessel function of first kind. Now consider a general wideband RF input signal $Z(t) = \sum_k \rho_k(t)\sin(\omega_k t + \vartheta_k(t))$ with multiple frequency components ω_k. Distinct from systems in which the aggregate collection of channels is collectively detected (e.g. SCM systems), we consider here the use of an optical filter bank to select the first order upper sideband of each ω_k. The detected electrical signal $S_k(t)$ after coherent downconversion can be derived as

$$S_k(t) = \prod_{p \neq k} J_0(\beta\rho_p) \cdot J_1(\beta\rho_k)\sin(\omega_{IF}t + \vartheta_k(t)) \tag{2}$$

Terms up to 4th order are included in Equation (2). Comparing Equations (1) and (2) it is seen that the first product term modulates the response and represents the nonlinear distortion due to XGM, while the $J_1(\beta\rho_k)$ term represents IMD. As an example, consider an RF input signal with four tones, two tones each centered on frequency ω_1 and ω_2. In this case $\vartheta_k(t) = 0$. We can write $Z(t) = 2\beta\, x_0 \cos(\delta_1 t)\sin(\omega_1 t) + 2\beta\, y_0 \cos(\delta_2 t)\sin(\omega_2 t)$, where the four tones are at $(\omega_2 \pm \delta_2)$ and $(\omega_1 \pm \delta_1)$. Consider the signal at ω_2 and how it is impacted by by a strong interferer at ω_1 after filtering. The response after the optical filter at frequency ω_2 is given by

$$E(t)\big|_{\omega_2} \propto J_0(2\beta\, x_0 \cos(\delta_1 t))J_1(2\beta\, y_0 \cos(\delta_2 t))\sin(\omega_2 t)$$
$$\sim \left[\left(1-\frac{\beta^2 x_0^2}{2}\right)+\frac{\beta^2 x_0^2}{2}\cos(2\delta_1 t)\right]\left[\beta\, y_0 \cos(\delta_2 t)\sin(\omega_2 t)\right] \quad (3)$$

Equation (3) shows that XGM produces images (sidebands) of the original signal offset by $\pm 2\delta_1$ whose intensity varies as $(\beta x_0)^2$.

The effects of IMD and XGM can be mitigated in systems where all signals $S_k(t)$ are recorded. The system of equations in Equation (2) are readily solved for $\rho_k(t)$ using the Newton's method or Levenberg–Marquardt algorithm. In this analysis the sinusoidal term in Eq. (3) was removed by traditional carrier recovery. These methods are particularly effective since the Jacobian has an analytical representation. The Jacobian is well conditioned as long as $\frac{d}{d\rho} J_1(\rho_k) > 0$.

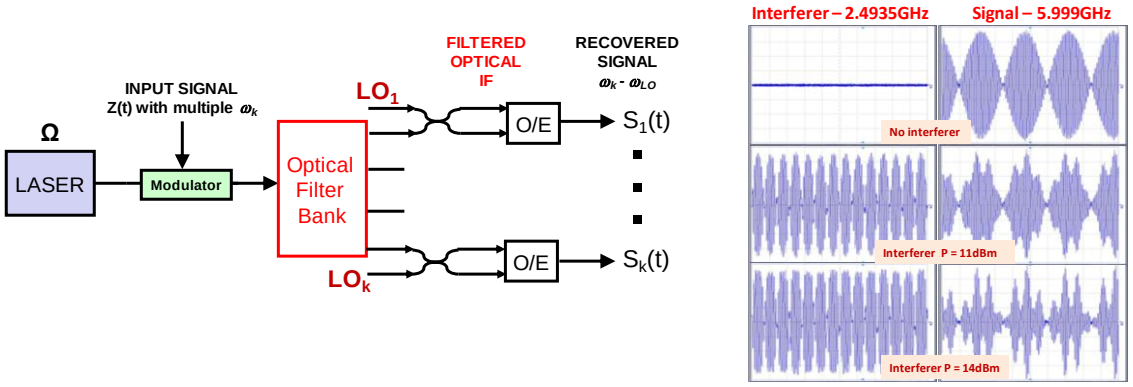

Fig. 1: (a) Optically filtered coherent analog multi-channel photonic system. (b) Time-domain waveforms for signal and strong interferer tones showing considerable distortion on signal tones.

3. Experimental setup and results: The experimental setup is similar to that shown in Fig. 1(a). We use four tones (two tones each in two frequency bands) to emulate a wideband input RF signal. The four tones are generated from four synthesizers and passively combined before being amplified by the modulator driver amplifier.

The output power of a 1550nm laser is first amplified to 16 dBm and then split between the signal and the LO paths for phase modulation. The input RF signal Z(*t*) is four tones, two tones each for the signal and the interferer. The two tones for the signal are at frequencies 5.997 GHz and 6.001 GHz spaced by $2\delta_2$ = 4 MHz, while the interferer tones are at frequencies 2.490 GHz and 2.497 GHz spaced by $2\delta_1$ = 7 MHz. The power level for the signal and interferer tones can be varied with an attenuator. After being passively combined, the four tones are split and then each is amplified using an RF amplifier (P_{1dB} = +21dBm, OIP_3 = +30dBm) for complementary drive to a dual-drive LiNbO3 MZM. The modulator is biased for carrier suppression, which also advantageously suppresses all even-order sidebands. A fifth synthesizer provides the LO RF signal at ω_{LO} = 6.049 GHz to downconvert the signal band. The phase modulated optical signals are combined after which a narrowband optical filter with a 3-dB bandwidth of 350 MHz filters the upper sideband centered at 6 GHz, presenting >20 dB suppression to the interferer channels at ~2.5 GHz. For each frequency band the output is coherently detected by tuning the LO frequency to either 6.049GHz or 2.5435GHz, resulting in the recovered signal *S*(*t*) centered at an IF of ω_{IF} = 50 MHz. The detected signal is monitored on an RF spectrum analyzer and recorded with a 20GSa/s real-time scope (8 bit ADC resolution without averaging, 2.5 GHz BW). The end-to-end optical loss was calibrated for each measurement.

In Fig. 2(a) we plot the power of the fundamental (triangles) and IMD3 (squares) as a function of modulator drive power for both signal (solid symbols) and interferer (open symbols) when each is present individually. As

expected, in each case the fundamental and the IMD3 show the characteristic response with slopes of one and three respectively. The dotted line shows the suppression previously derived [2] of IMD3 though postcompensation that can be obtained by inverting the response of Eq. (1) when only a single frequency band is present. Next we consider the case when both signal and interferer tones are present. Figure 2(b) plots the power of the fundamental for the signal and the power in the XGM sidebands at frequency ($\omega_2 + \delta_2 + 2\delta_1$) (see Eq. (3)) as the interferer tones power levels is changed. It is clearly seen that when both frequency bands are present simultaneously, the sidebands due to XGM grow with a slope of two, while the gain of the fundamental is compressed. Post-processing was next applied. The resulting sideband power is suppressed by 25-30dB and is also plotted in Fig. 2(b) (open squares). Figure 3(a) shows the postcompensation corrected time-domain waveforms for the signal tones. Also shown for comparison are the undistorted signal waveforms (when no interferer is present) and the distorted signal due to XGM. The corrected waveform closely follows the undistorted signal waveforms. The corresponding RF spectrum shown in Fig. 3(b) illustrates ~30dB XGM sideband suppression and ~20dB IMD3 suppression after postcompensation.

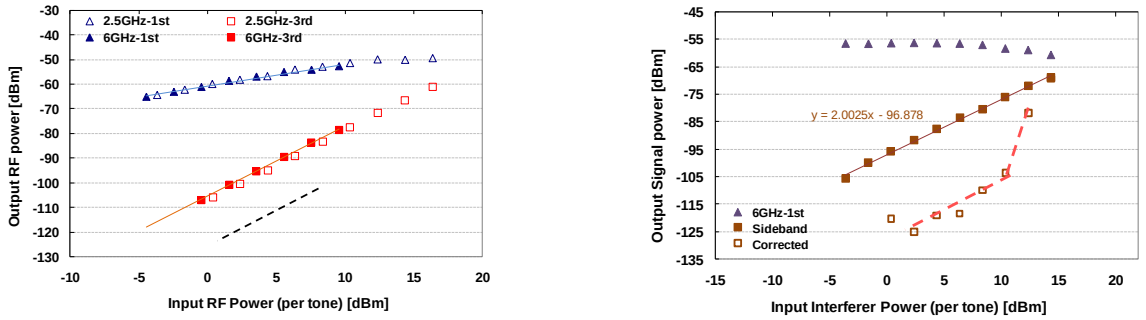

Fig. 2: (a) Fundamental and IMD3 as a function of input RF power for signal (solid symbols) and interferer (open symbols) when each is present individually. (b) Signal fundamental and XGM sideband as a function of input interferer power.

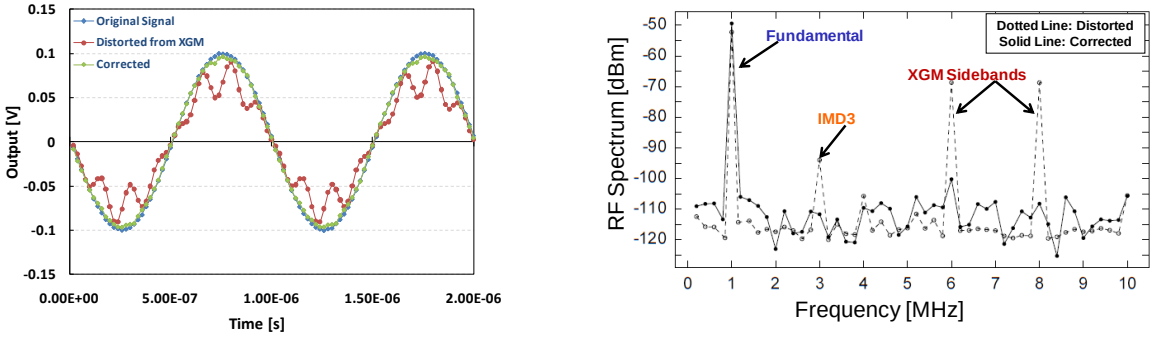

Fig. 3: (a) Time-domain waveforms for signal tones showing the original signal, distorted signal due to XGM and postcompensation corrected signal. (b) RF spectrum showing the fundamental and XGM sidebands before (dotted line) and after (solid line) postcompensation correction.

4. Conclusions: We have analyzed the impact of nonlinearity due to cross-gain modulation in wideband filtered multi-channel analog photonic systems and experimentally demonstrated the suppression of XGM sidebands and third-order IMD using post-processing that is based on inverting the link response. These methods, while effective, are highly sensitive to gain calibration error.

This material is based upon work supported by the Defense Advanced Research Projects Agency PhASER program under Contract No. HR0011-08-C-0026. The views, opinions, and/or findings contained in this article are those of the authors and should not be interpreted as representing the official views or policies, either expressed or implied, of the Defense Advanced Research Projects Agency or the Department of Defense.

References

[1] K. Takada, et. al. "1-GHz-Spaced 16-Channel Arrayed Waveguide Grating for a Wavelength Reference Standard in DWDM Network Systems," IEEE J. Lightwave Technology 20(5), 850-853 (2002).

[2] T. Banwell et. al., "Analytical expression for large signal transfer function of an optically filtered analog link," Optics Express 17, 15449–15454 (2009).

[3] G.E. Betts, "Linearized modulator for suboctave-bandpass optical analog links," IEEE Transactions on Microwave Theory and Techniques 42, 2642-2649 (1994).

[4] A. Ramaswamy, et. al., "Integrated coherent receivers for high-linearity microwave photonic links," J. of Lightwave Technology 26, 209-216 (2008).

[5] T.R. Clark, M.L. Dennis, "Coherent optical phase modulation link," IEEE Photonics Technology Letters 19, 1206-1208 (2007).

[6] Mary R. Phillips, Thomas E. Darcie, "Lightwave Analog Video Transmission," Chapter 14 in *Optical Fiber Telecommunications IIIA*, Academic Press, (1997).